(昭和55年11月　日本造船学会秋季講演会において講演)

Characteristics of Free Surface Shock Waves around Wedge Models

by Masayuki Takahashi*, *Member*　　Hisashi Kajitani**, *Member*
Hideaki Miyata**, *Member*　　Makoto Kanai**

Summary

Characteristics of free surface shock waves are experimentally investigated with wedge models, which clarify the ways how the occurrence of free surface shock waves at the bow is ruled by velocity of advance, draft and entrance angle. The variation of shock angle is very similar to that of shock waves in shallow water. Application of nonlinear shallow water theory is attempted by introducing equivalent shallow water depth that connects shock waves in deep water with those in shallow water. The estimations of shock angle and resistance due to free surface shock waves turn out successful for the improvement of hull forms.

1. Introduction

The authors have verified the existence of a kind of shock wave in the near-field of ships in translational motion in deep water, and named these waves as Free Surface Shock Waves (abbreviated as FSSW hereafter).[1)2)3)] The characteristics of FSSWs and their effects have been explained with extensive experimental results.[8)]

The occurrence of nonlinear waves cannot be explained by the linear wave making theory. It should be explained by the solution of a nonlinear partial differential equation. Baba[6)] and Takekuma[7)] first noticed the necessity of introducing nonlinear partial differential equation in terms of the wave breaking phenomena. However the successive development of their works could not have been expected until it is clarified by the authors that the essence of the nonlinear flow phenomena in the near-field is the occurrence of FSSWs instead of wave breaking.

In our previous works tested models have been ship models, and the occurrence of FSSWs is rather complex. Therefore, in this paper, fundamental characteristics of FSSWs are systematically analysed with wedge models whose length is about 1 m. One of the most significant FSSWs occurs around the bow and it is principally effected by bow forms. With these simple models, fundamental characteristics are expected to be found out clearly. In the near-field of the models, wave pattern measurement and disturbance velocity measurement are carried out, in which draft of model, velocity of advance and entrance angle are considered as main parameters for FSSWs. The parameters are varied in the ranges of $1\,\text{cm} \leq d \leq 15\,\text{cm}$, $0.5\,\text{m/s} \leq V \leq 2.0\,\text{m/s}$ and $5° \leq \alpha \leq 25°$.

In chapter 3, quantitative properties of FSSWs, i.e., wave height, shock angle and discontinuity in velocity are examined, and their resemblance to shallow water shock waves is discussed. In chapter 4, equivalent shallow water depth is introduced which enables us to apply the nonlinear shallow water theory. The law of similarity that governs FSSWs is also discussed. In chapter 5, some practical methods for the explanation of the occurrence of FSSWs and for the estimation of resistance due to FSSWs are presented.

2. Nomenclature

B	beam length
C_w	wave making resistance coefficient derived from towing test
C_{wp}	D_0 derived from wave analysis
C_{ws}	resistance coefficient due to free surface shock wave
d	draft of ship
F_d	Froude number based on d
F_h	D_0 based on h_1

* Nippon Kokan K.K.
** The University of Tokyo

$F_{\tilde{h}}$ $D_{\underline{Q}}$ based on $\tilde{h}_1$
F_n $D_{\underline{Q}}$ based on L
g acceleration of gravity
h shallow water depth
$\tilde{h}_1$ equivalent shallow water depth
h_0 stagnation depth, total head $gh_1+V^2/2$ or $g\tilde{h}_1+V^2/2$
L length between perpendiculars
u, v, w velocity components in x, y and z directions, respectively
V (without subscripts) velocity of uniform stream$=V_1$
V (with subscripts) velocity components in horizontal plane (see Fig. 8)
x axis parallel to ship centerline, aftward positive
y axis parallel to ship beam
z axis vertical
α entrance angle
β shock angle
ζ wave height
ρ density of water

superscripts

— non-dimensionalized by $\sqrt{(2/3)gh_0}$
~ equivalent to the case in shallow water

subscripts

n normal to shock front
t tangential to shock front
1 ahead of shock front
2 behind shock front

3. Characteristics of free surface shock waves

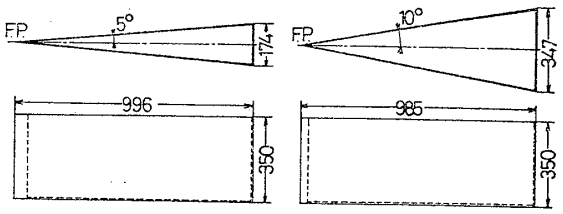

Fig. 1 Wedge model

Three wedge models are produced, i.e., two whose α is 10° and one whose α is 5° as are shown in Fig. 1. They can be combined into wedge models whose α is 15°, 20° and 25°.

3.1 Wave profile

In Fig. 2 photographed wave patterns are shown in which the dependence of shock angle on draft, velocity of advance and entrance angle is clearly observed. Shock angle, that is, the angle of wave crest to the centerline of the model, is expressed as a function of the three parameters, which is one of the significant characteristics of FSSW. In Fig. 3, measured wave profiles on the line parallel to the centerline of the model are shown, the origin being at F.P. As the draft or entrance angle increases, the phase of wave profile goes ahead and simultaneously the wave height increases. With the decrease of advance velocity the phase of the wave advances. This property is entirely different from that of linear dispersive waves. The forward advance of the wave crest means increase of shock angle. Therefore, it is noticed that the increase of shock angle

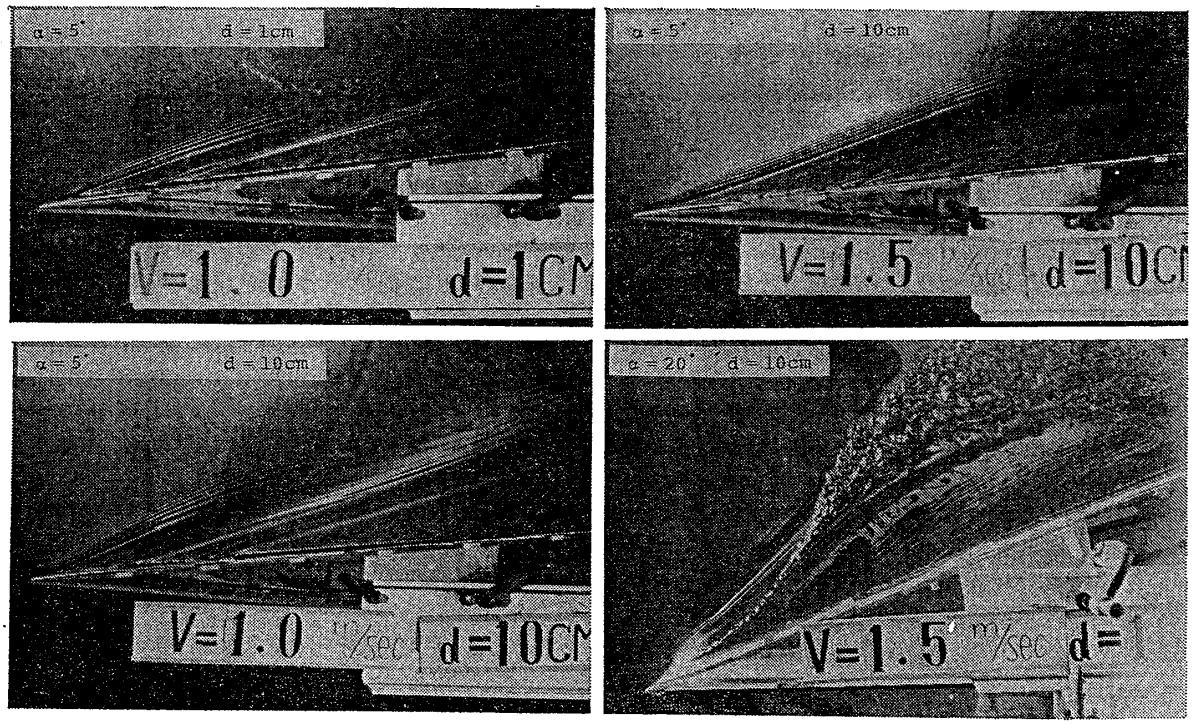

Fig. 2 Wave pattern around wedge models

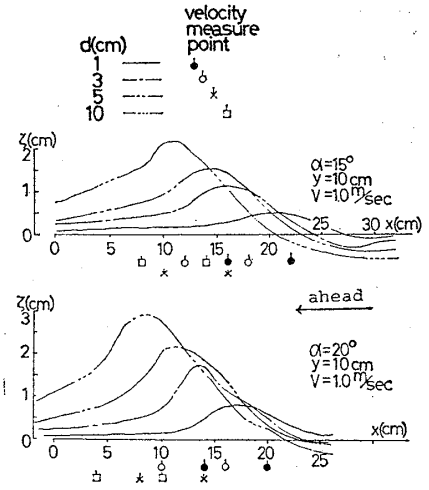

Fig. 3 Measured wave profile

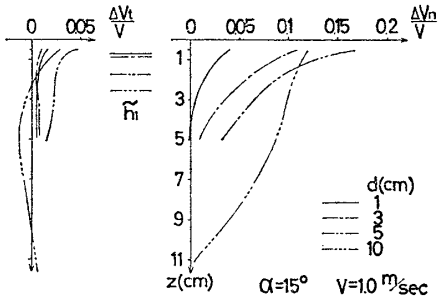

Fig. 4 Velocity change across shock front

is usually accompanied with the increase of wave height. The increase of shock angle is generally increase of the strength of discontinuity by FSSWs, and the strength of discontinuity is revealed in wave height in Fig. 3.

3.2 Discontinuity

Measurement of velocity components is undertaken by a five-hole pitot tube at 3 cm fore and back of the shock front line. The change of velocity across the front is separated into components parallel and normal to the wave front. An example is shown in Fig. 4, in which the change of velocity components satisfies the shock condition, that is, $\Delta V_t = 0$ and $\Delta V_n \neq 0$. It is also clarified that discontinuity in velocity is limited within the thin layer adjacent to the free surface. Basic properties of FSSWs which are found out on ship models are ascertained by wedge models.

3.3 Variation of shock angle

The experimental relation between shock angle and entrance angle is put in order in Figs. 5, 6 and 7 with the three parameters. The shock angle increases with the increase of entrance angle, with the decrease of advance velocity and also with the increase of draft. These relations are quite systematic and it implies the

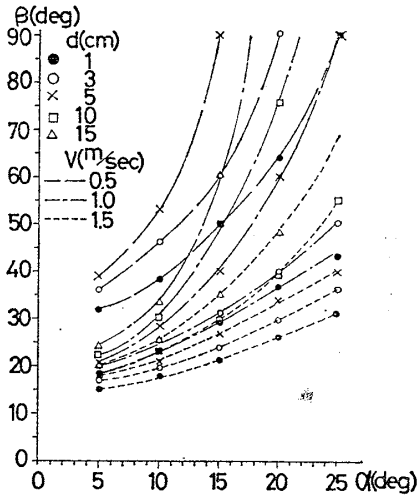

Fig. 5 Measured α–β relation

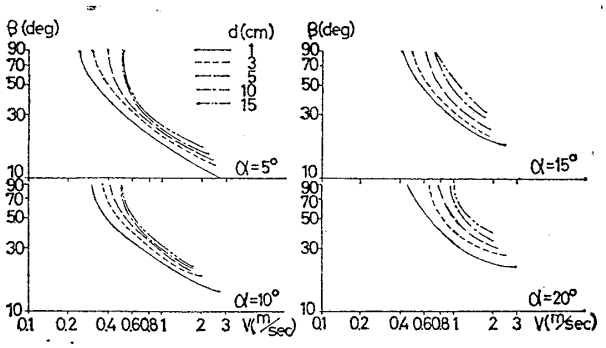

Fig. 6 Variation of shock angle (a)

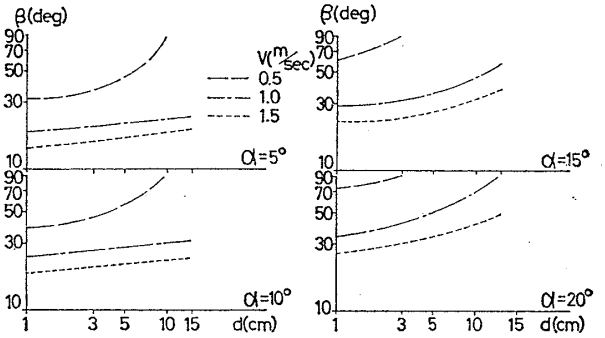

Fig. 7 Variation of shock angle (b)

role and the presence of a critical speed. Two kinds of shock wave are recognized; one is normal shock wave whose shock angle is 90°, and the other is oblique shock wave. Normal shock wave abruptly changes into oblique one with the increase of velocity. In Figs. 6 and 7 shock angle of both normal and oblique shock wave is recorded, and they show rapid change in shock angle on the process of transition from normal to oblique.

The above mentioned relations are very similar to that of a point disturbance in shallow water

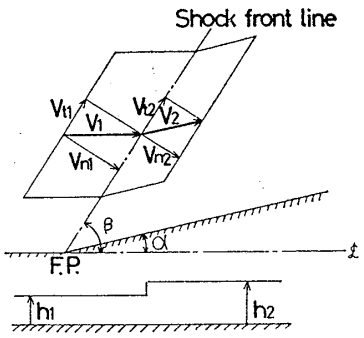

Fig. 8 Sketch for the problem of nonlinear shallow water wave

which advances at V and generates waves that propagate at the speed of $\sqrt{gh}$. The shock angle is determined simply as $\sin^{-1}(\sqrt{gh}/V)$.

For more thorough explanation of α–β relation in Fig. 5, the theory for shallow water shock waves on a two-dimensional wedge model is introduced. Suppose viscosity and compressibility of water and vertical acceleration are neglected, the conservation of mass is,

$$h_1 V_{n1} = h_2 V_{n2} \qquad (1)$$

and that of momentum is,

$$h_1 V_{n1}^2 + g\frac{h_1^2}{2} = h_2 V_{n2}^2 + g\frac{h_2^2}{2}$$

for normal component (2)

$$V_{t1} = V_{t2} \quad \text{for tangential component} \qquad (3)$$

As a consequence, the relation between α and β is as follows.[5]

$$\tan\alpha = \frac{\tan\beta(\sqrt{1+8F_h^2\sin^2\beta}-3)}{2\tan^2\beta - 1 + \sqrt{1+8F_h^2\sin^2\beta}} \qquad (4)$$

where $F_h \equiv V/\sqrt{gh_1}$

This relation is shown in Fig. 9.

The qualitative resemblance of Fig. 9 to Fig. 5 is astonishing. This resemblance is another verification of the existence of shock waves in deep water. The formation of linear dispersive waves does not depend on draft nor entrance angle.

In Fig. 9, α–β relation for only oblique shock waves is present and we will concentrate our attention on oblique shock waves in this paper, for oblique FSSWs mostly contribute to ship resistance at service speed.

4. Equivalent shallow water depth

4.1 Definition of equivalent shallow water depth

Theoretical explanation of the occurrence and effect of FSSWs is very difficult, because the governing equation is nonlinear and the nonlinearity plays a decisive role. Therefore, some

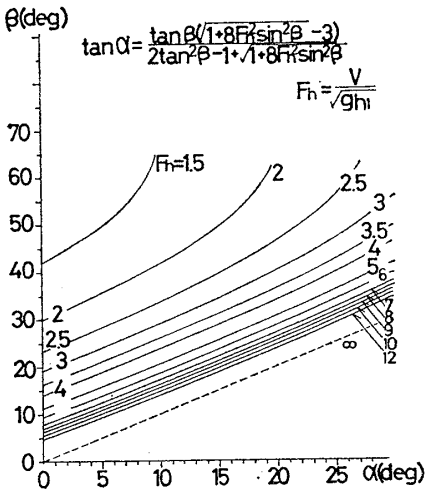

Fig. 9 α–β relation by nonlinear shallow water theory

simplification of the problem should be pursued. This will be a practical approach for the finding of some guidelines for hull form design. In this paper simplification is attempted by introducing equivalent shallow water depth which changes the problem in deep water into that in shallow water, which was once tried by Baba for a one-dimensional case. The flow with discontinuity is limited in the thin layer adjacent to the free surface, and therefore, we assume that the flow in this thin layer is ruled by equations for shock waves in shallow water. The difference in characteristics between FSSWs and shallow water shock waves is adjusted by the definition of equivalent shallow water depth. In other words, equivalent shallow water depth is defined so that the explanation of the flow in the equivalent depth by the nonlinear shallow water equations accords with experimental facts.

Thus, equivalent shallow water depth is defined with measured values. We choose α, β, and V for this purpose. Wave height can also be the parameter, but it is excluded because of the arbitrariness. Fig. 5 is the experimental α–β–V relation for FSSWs and Fig. 9 is the theoretical α–β–F_h relation for shallow water shock waves. Figs. 5 and 9 are overlapped and $F_{\tilde{h}}$ for FSSWs is determined at each conditions. In consequence equivalent shallow water depth is obtained from the following relation.

$$\tilde{h}_1 = \frac{1}{g}\left(\frac{V}{F_{\tilde{h}}}\right)^2 \qquad (5)$$

Calculated $\tilde{h}_1$ is figured in Figs. 10 to 13. Figs. 10 and 11 show that $\tilde{h}_1$ is approximately independent of advance velocity and that it increases with the increase of draft. Fig. 12 shows the dependence on α. The ratio of $\tilde{h}_1$ to

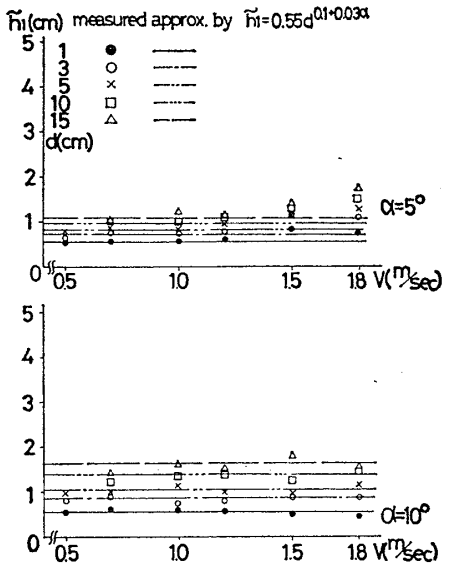

Fig. 10 Dependence of equivalent shallow water depth on velocity (a)

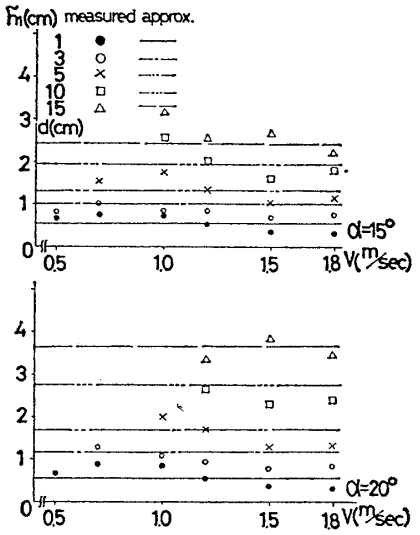

Fig. 11 same as Fig. 10 (b)

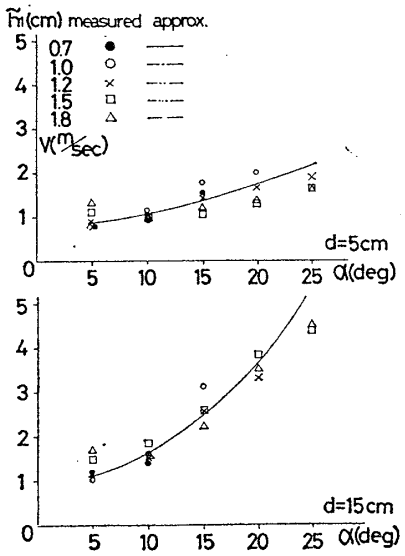

Fig. 12 Dependence of equivalent shallow water depth on entrance angle

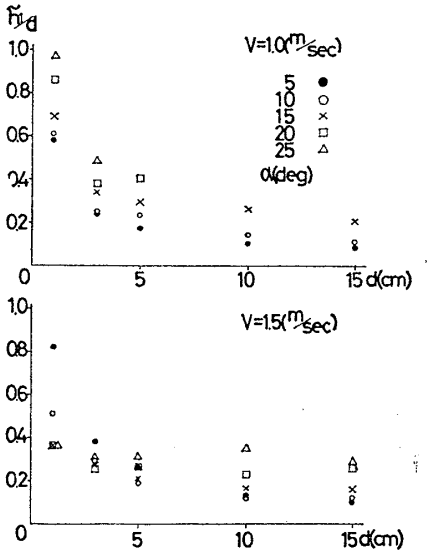

Fig. 13 Dependence of equivalent shallow water depth on draft

draft ($\tilde{h}_1/d$) is shown in Fig. 13, in which it is noted that the ratio is not constant in the shallow-draft region, however, it is saturated and becomes constant in the relatively deep-draft region. The variation of $\tilde{h}_1$ qualitatively accords with the thickness of the thin layer measured. This relation can be summed up into the following simple formula.

$$\tilde{h}_1 = 0.55 d^{0.1+0.03\alpha} \qquad (6)$$

($\tilde{h}_1$, d in cm, α in degree)

This empirical relation is valid within the ranges $5° \leq \alpha \leq 25°$, $1\text{ cm} \leq d \leq 15\text{ cm}$ and $0.5\text{ m/s} \leq V \leq 1.8\text{ m/s}$.

4.2 Law of similarity for free surface shock waves

Law of similarity is always a great problem to be examined. On the present problem law of similarity for FSSW can be studied by examination of the law for $\tilde{h}_1$. Equation (6) which is valid within a restricted range implies a non-linear relation between $\tilde{h}_1$ and d, and consequently, Froude's law of similarity is violated. However, $\tilde{h}_1$ is proportional to d in deeper draft region as is shown in Fig. 13. This proportional relation leads to the following equations.

$$F_{\tilde{h}} = \frac{10}{\sqrt{5+\alpha}} F_d \qquad (\alpha \text{ in degree}) \qquad (7)$$

$$\tilde{h}_1 = (5+\alpha)/100 \cdot d \qquad (7')$$

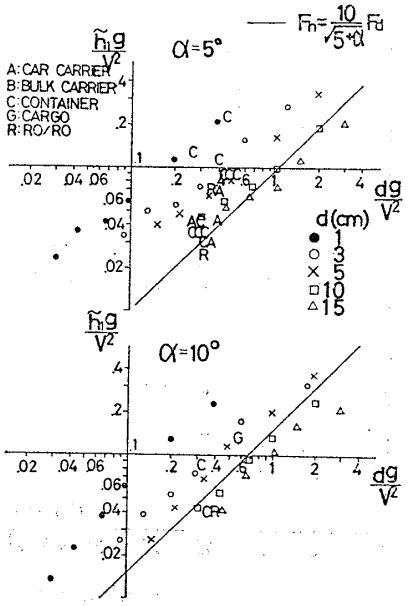

Fig. 14 Relation between $\bar{h}_1$ and d

In the region where equation (7) holds Froude's law of similarity is maintained in a slightly different fashion. Nondimensional relation between $\bar{h}_1$ and d obtained from experiments is shown in Fig. 14 together with the lines expressed by equation (7). The relation (7) is approximately satisfied except for extremely shallow drafted conditions. Equation (7) is rewritten as,

$$F_{\bar{h}}=\frac{10}{\sqrt{5+\alpha}}\sqrt{\frac{L}{d}}F_n \qquad (8)$$

Thus, usual Froude number is in proportional relation with $F_{\bar{h}}$ for a fixed entrance angle, and therefore, shock angle defined by equation (4) remains constant in case F_n is kept constant. In Fig. 14 $\bar{h}_1$ for full-scale ships is plotted in English capitals, which is estimated from β measured in photos. Although the measurement of β is rather rough, the relation expressed by (7) or (8) seems to be valid to a certain degree.

The law of similarity has been examined in terms of shock angle only. It must also be examined with other physical values such as wave height, and it is still left vague, which requires urgent investigation. However, the relation between shock angle and wave height is qualitatively simple as is shown in Fig. 3. The decrease of shock angle is accompanied with the decrease of wave height and the improvement of hull forms can be achieved by the decrease of shock angle. Therefore, the law of similarity in terms of shock angle described above is very basic and important for further investigations.

5. Application of nonlinear shallow water theory

Equivalent shallow water depth is defined and FSSWs become to be approximately explained by the theory of nonlinear shallow water flow whose depth is $\bar{h}_1$. Assume $\bar{h}_1$ or $F_{\bar{h}}$ is determined by equation (6) or (7), some of the methods for shallow water shock waves are applicable to the problems of FSSW.

5.1 Calculation of free surface shock wave resistance

The theory of shallow water shock waves by Preiswerk[4] is applied to the problem of FSSW. From the equations of conservation of mass (1) and of that of momentum (2) (3), the relation of shock polar in hodograph plane is derived as follows:

$$\bar{v}_2^2=(\bar{u}_1-\bar{u}_2)\left(\bar{u}_2-\bar{u}_1\sqrt{\frac{3-\bar{u}_1^2}{3-4\bar{u}_1\bar{u}_2+3\bar{u}_1^2}}\right) \qquad (9)$$

Variables with bars indicate values nondimensionalized by $\sqrt{(2/3)[gh_1+(V^2/2)]}$. Equation (9) constitutes so-called shock polar contours shown in Fig. 15, in which the points where contours cross $\bar{u}$-axis at the right-hand side are velocity of uniform flow. The velocity vector behind the shock front is obtained as a crossing point of the contour with the straight line whose gradient is $\tan\alpha$, when h_1 is constant. For FSSWs whose $\bar{h}_1$ depends on α, the shock polar is deformed as is shown by plotted marks in Fig. 15 for various draft conditions.

Velocity vectors behind FSSWs estimated in Fig. 15 are compared with measured vectors in Fig. 16. The starting points of the arrows indicate experimental value, while the head of the arrow indicate theoretical value. The agreement is not satisfactory for shallow drafted conditions and for models with large entrance angle. The disagreement is mainly because the flow around FSSWs is not exactly two-dimensional and the flow behind the shock front is not always parallel

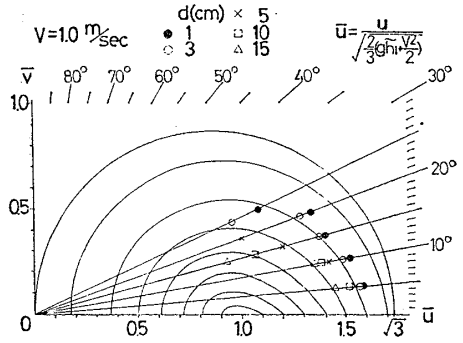

Fig. 15 Theoretical shock polar in hodograph plane

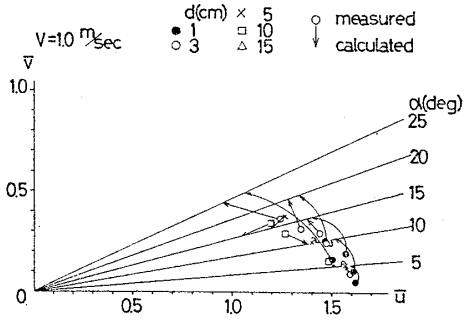

Fig. 16 Measured velocity change

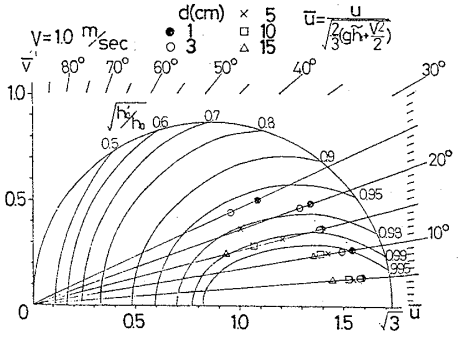

Fig. 17 Contours of constant stagnation depth

to the wall of the model.

The total head behind the shock front h_0' is obtained by the following equation.

$$\frac{h_0'}{h_0}=\sqrt{\left(\frac{h_1}{h_0}\right)^2+\frac{4}{3}\bar{u}_1(\bar{u}_1-\bar{u}_2)\left(\frac{h_1}{h_0}\right)}+\frac{1}{3}(\bar{u}_2^2+\bar{v}_2^2) \tag{10}$$

The energy loss ΔE and the rate of energy loss Δe are,

$$\Delta E=mg\left(\frac{h_0}{2}-\frac{h_0'}{2}\right)=mg\frac{h_0}{2}\left(1-\frac{h_0'}{h_0}\right) \tag{11}$$

$$\Delta e=\Delta E/E=1-h_0'/h_0 \tag{12}$$

in which mg is amount of flow per unit time.

Equi-total-head contours are drawn in hodograph plane in Fig. 17. The values on the contours show $\sqrt{h_0'/h_0}$, and small value means great energy loss by shock waves.

As often happens, C_w curves have remarkable humps in low Froude number range for shallow drafted ships, whereas C_{wp} curves do not. These humps that cannot be grasped by wave analysis will be explained by the above described estimation of resistance due to FSSWs, when h_1 is replaced by $\tilde{h}_1$.

An example for two bulk carriers on ballast condition is present in Fig. 18. The shock angle is measured in wave pattern photos and mg is assumed to be $2b\tilde{h}_1V\rho g$, while width of discontinuity b is intuitively decided in the wave pattern photos. Broken lines are estimated resistance coefficient curves due to FSSWs. Curves designated by A are C_{ws} by the first FSSW and those designated by B are by the second FSSW. Bulk 2 has a prominent hump around $F_n=0.15$, while Bulk 1 does not. The broken line designated by B for Bulk 2 qualitatively explains the hump around $F_n=0.15$. Although there left many problems for precise quantitative estimation of C_{ws}, the hump of C_w in Fig. 18 is the hump in C_{ws} without doubt and the present method seems to be applicable.

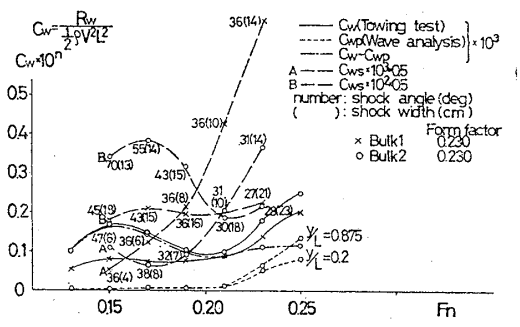

Fig. 18 Wave resistance curves of bulk carriers on ballast condition

5.2 Method of characteristics

Method of characteristics briefly explained in reference 3) is applied to the scheme of hull form improvement in a little more consistent manner. The governing equation of the nonlinear shallow water waves is,

$$\left(1-\frac{\phi_x^2}{gh}\right)\phi_{xx}-2\phi_{xy}\frac{\phi_x\phi_y}{gh}+\left(1-\frac{\phi_y^2}{gh}\right)\phi_{yy}=0 \tag{13}$$

where, $u=\phi_x,\ v=\phi_y$

For FSSWs h is replaced by $\tilde{h}_1$. In supercritical region equation (13) is a hyperbolic partial differential equation, and the method of characteristics can be applied, Equation (13) is rewritten by Legendre transformation $\chi=ux+vy-\phi$ into,

$$\left(1-\frac{u^2}{gh}\right)\chi_{vv}+2\chi_{uv}\frac{uv}{gh}+\left(1-\frac{v^2}{gh}\right)\chi_{uu}=0 \tag{14}$$

where, $x=\chi_u,\ y=\chi_v$

From this transformation the lines of characteristics in hodograph plane $\Gamma_\pm$ are tangential to the epicycloids whose radius of the rotating circle is $(\sqrt{3}-1)/2$ and that of the fixed circle is 1. The characteristic lines in physical plane $C_\mp$ are normal to $\Gamma_\pm$ respectively. Thus, $C_\mp$ are normal to the epicycloids. The lines of characteristics $\Gamma_\pm$ and $C_\mp$ are expressed as follows, respectively.

$$\left(\frac{dv}{du}\right)_{\Gamma_\pm}=\frac{uv/g\tilde{h}_1\pm\sqrt{(u^2+v^2)/g\tilde{h}_1-1}}{1-v^2/g\tilde{h}_1} \tag{15}$$

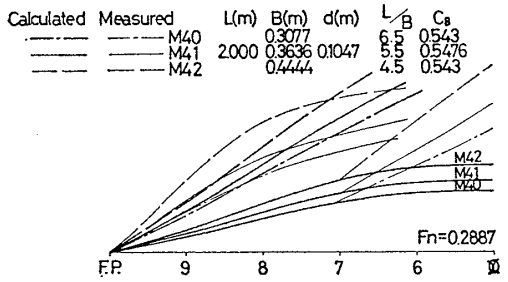

Fig. 19 Shock front lines of M40 beam–length series

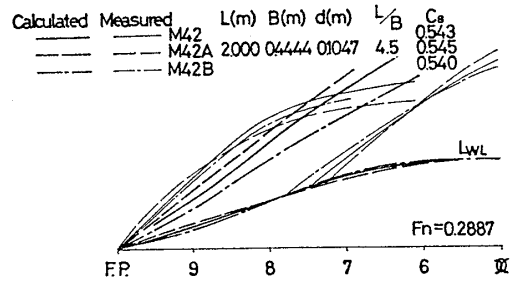

Fig. 20 Shock front lines of M42 sectional area curve series

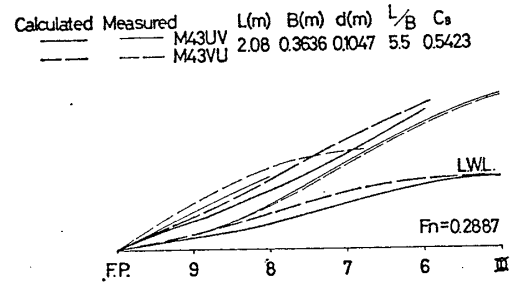

Fig. 21 Shock front lines of M43 frame line series

$$\left(\frac{dy}{dx}\right)_{C_{\mp}}=\frac{-uv/g\tilde{h}_1\pm\sqrt{(u^2+v^2)/g\tilde{h}_1-1}}{1-u^2/g\tilde{h}_1} \qquad (16)$$

Lines of characteristics for model ships are calculated in this way, assuming that the starting point of the epicycloid, which means the uniform flow, is determined by $\tilde{h}_1$ and velocity of advance and that the hull forms are represented by the water lines which are expressed by successions of straight lines. Thus, lines of characteristics in physical plane are successively obtained. The curve connecting the points where lines of characteristics cross each other is the shock front line.

This method is applied to some ship models. Calculated examples are present in Figs. 19 to 21. Qualitative agreement between experimental results and the present theoretical interpretations is excellent in all the three cases for the first FSSWs. This method of characteristics may be effective for hull form improvement, because the agreement of estimated shock angle is excellent in qualitative sense and the decrease of shock angle straightly means decrease of resistance due to FSSWs.

This method, however, has some defects; that is, 1) it cannot estimate second FSSWs which receive effects by the first ones and 2) it cannot be applied to V–shaped hull forms or hulls with bulb, because hull forms are represented by load water lines at present. These defects should be remedied for the further development of the new design procedure.

6. Conclusion

Principal conclusions are as follows.

1) Characteristics of free surface shock waves are systematically clarified. The effects of draft and entrance angle of ships and advance velocity on the generation of free surface shock waves are put in order.

2) The change of shock angle and wave height around bow shows close resemblances to shallow water shock waves.

3) The law of similarity for free surface shock waves is examined. They are approximately ruled by Froude number based on draft.

4) Experimentally introducing the concept of equivalent shallow water depth, the authors present two practical methods for the qualitative estimation of free surface shock wave resistance and of shock wave formation.

Acknowledgement

This research is partially supported by the Grant–in–Aid for Scientific Research of the Ministry of Education, Science and Culture, and also by the Kawakami Foundation.

Reference

1) T. Inui, H. Kajitani, H. Miyata: Experimental Investigations on the Wave Making in the Near–Field of Ships, J. of the Kansai Soc. of Naval Arch., Japan, Vol. 173 (1979) (English).

2) T. Inui, H. Kajitani, H. Miyata, M. Tsuruoka, A. Suzuki, T. Ushio: Non–Linear Properties of Wave Making Resistance of Wide-Beam Ships, J. of the Soc. of Naval Arch. of Japan, Vol. 146 (1979) (English).

3) H. Miyata, T. Inui, H. Kajitani: Free Surface Shock Waves around Ships and Their Effects on Ship Resistance, J. of the Soc. of Naval Arch. of Japan, Vol. 147 (1980) (English).

4) E. Preiswerk: Anwendung Gasdynamischer Methoden auf Wasserströmungen

mit Freier Oberfläche, Mitt. Inst. Aerodynamik, Eidgen. Techn. Hochsch, Zürich, No. 7 (1938).

5) J. V. Wehausen, E. V. Laitone: Surface Waves, Handbuch der Physik, Vol. 9, Springer–verlag (1960).

6) E. Baba: A new Component of Viscous Resistance of Ships, J. of the Soc. of Naval Arch. of Japan, Vol. 125 (1969) (English).

7) K. Takekuma: Study on the Non–Linear Free Surface Problem around Bow, J. of the Soc. of Naval Arch. of Japan, Vol. 132 (1972) (English).

8) N. Kawamura, H. Kajitani, H. Miyata, Y. Tsuchiya: Experimental Investigation on the Resistance Component Due to Free Surface Shock Waves on Series Ship Models, to be presented to the autumn meeting of the Kansai Soc. of Naval Arch., Japan (1980) (English).